Huber, R., & Bennett, W. S. (1983) *Biopolymers 22*, 261–280.
Jardetzky, O., Akasakan, K., Vogel, R., Morris, S., & Holmes, K. C. (1978) *Nature (London) 273*, 564–566.
Karplus, M., & McCammon, J. A. (1983) *Annu. Rev. Biochem. 53*, 263–300.
Klug, A. (1979) *Harvey Lect. 74*, 141–172.
Nelson, H. C. M., Hecht, M., & Sauer, R. T. (1983) *Cold Spring Harbor Symp. Quant. Biol. 47*, 441–449.
Pabo, C. O., & Lewis, M. (1982) *Nature (London) 298*, 443–447.
Pabo, C. O., Sauer, R. T., Sturtevant, J., & Ptashne, M. (1979) *Proc. Natl. Acad. Sci. U.S.A. 76*, 1608–1612.
Pabo, C. O., Krovatin, W. Jeffrey, A., & Sauer, R. T. (1982) *Nature (London) 298*, 441–443.
Perkins, S. J., & Dwek, R. A. (1980) *Biochemistry 19*, 245–258.
Piantine, V., Sorensen, O. W., & Ernst, R. R. (1982) *J. Am. Chem. Soc. 104*, 6800–6801.
Rance, M., Sorenson, O. W., Bodenhausen, G., Wagner, G., Ernst, R. R., & Wüthrich, K. (1983) *Biochem. Biophys. Res. Commun. 117*, 479–485.
Sauer, R. T., & Anderegg, R. (1978) *Biochemistry 17*, 1092–2200.
Sauer, R. T., Pabo, C. O., Meyer, B. J., Ptashne, M., & Backman, J. C. (1979) *Nature (London) 279*, 396–400.
States, D. J., Haberkorn, R., & Ruben, P. R. (1982) *J. Magn. Reson. 48*, 286–292.
Wade-Jardetzky, N., Bray, R. P., Onover, W. W., Jardetzky, O., Geisler, N., & Weber, K. (1979) *J. Mol. Biol. 128*, 259–264.
Weiss, M. A., Karplus, K., Patel, D. J., & Sauer, R. T. (1983) *J. Biomol. Struct. Dyn. 1*, 151–157.
Weiss, M. A., Eliason, J. L., & States, D. J. (1984) *Proc. Natl. Acad. Sci. U.S.A.* (in press).
Wüthrich, K., Wider, G., Wagner, G., & Braun, W. (1982) *J. Mol. Biol. 15*, 311–319.

Articles

Conformational Transitions of Thioredoxin in Guanidine Hydrochloride†

Robert F. Kelley and Earle Stellwagen*

ABSTRACT: Spectral and hydrodynamic measurements of thioredoxin from *Escherichia coli* indicate that the compact globular structure of the native protein is significantly unfolded in the presence of guanidine hydrochloride concentrations in excess of 3.3 M at neutral pH and 25 °C. This conformational transition having a midpoint at 2.5 M denaturant is quantitatively reversible and highly cooperative. Stopped-flow measurements of unfolding in 4 M denaturant, observed with tryptophan fluorescence as the spectral probe, reveal a single kinetic phase having a relaxation time of 7.1 ± 0.2 s. Refolding measurements in 2 M denaturant reveal three kinetic phases having relaxation times of 0.54 ± 0.23, 14 ± 6, and 500 ± 130 s, accounting for 12 ± 2%, 10 ± 1%, and 78 ± 3% of the observed change in tryptophan fluorescence. The dominant slowest phase is generated in the denatured state with a relaxation time of 42 s observed in 4 M denaturant. Both the slowest phase observed in refolding and the generation of the slowest phase in the denatured state have an activation enthalpy of 22 ± 1 kcal/mol. These features of the slowest phase are compatible with an obligatory peptide isomerization of proline-76 to its cis isomer prior to refolding.

The thioredoxin isolated from *Escherichia coli* contains 108 amino acid residues located in a single polypeptide chain having a single intrachain disulfide bond (Holmgren, 1968). Crystallographic analysis of the protein reveals it to contain a single twisted β-sheet composed of five strands flanked by four α-helical segments (Holmgren et al., 1975). These elements are integrated in a supersecondary structural array called the NAD binding domain, which has been observed to occur in a large number of proteins of diverse function. Since thioredoxin is the smallest monomeric protein known to contain an NAD binding domain, we consider it to be an excellent model protein for detailed studies of polypeptide chain folding. This paper describes equilibrium and kinetic measurements of the major conformational transition of *E. coli* thioredoxin using guanidine hydrochloride (Gdn-HCl)[1] as the denaturant at neutral pH. The majority of measurements were obtained with the protein having its single intrachain disulfide intact, a form we have denoted as oxidized thioredoxin. The principal novel observation is that the majority of the denatured protein refolds with a very long relaxation time, which likely results from the presence of a cis proline peptide bond in the native conformation.

Experimental Procedures

Materials. Thioredoxin was initially purified from *E. coli* B cells that were grown on minimal media and harvested at midlog phase by Grain Processing Corp. of Muscatine, IA. More recently the protein was purified from an *E. coli* strain constructed by Lunn et al. (1984) containing multiple copies of a plasmid with the gene for thioredoxin, which results in the cellular overproduction of thioredoxin by several hundred fold. Thioredoxin activity was measured by using the NADPH oxidation assay described by Laurent et al. (1964) and *E. coli*

† From the Department of Biochemistry, University of Iowa, Iowa City, Iowa 52242. *Received December 28, 1983.* This investigation was supported by U.S. Public Health Service Research Grant GM-22109 from the Institute of General Medical Sciences and by Program Project Grant HL-14388 from the National Heart, Lung and Blood Institute.

[1] Abbreviation: Gdn-HCl, guanidine hydrochloride.

0006-2960/84/0423-5095$01.50/0

thioredoxin reductase, which initially was a gift of Å. Holmgren (Stockholm, Sweden) and more recently was prepared by the affinity procedure of Pigiet & Conley (1977). Thioredoxin concentration was determined by absorbance measurements at 280 nm using an extinction coefficient of 13.7 mM^{-1} cm^{-1} (Reutimann et al., 1981). Thioredoxin was purified by a modification of the procedure of Holmgren & Reichard (1967). Modifications included (i) elimination of the acid precipitation step, (ii) heating the streptomycin supernatant for 5 min at 70 °C instead of 80 °C, (iii) concentration of the heated supernatant by hollow fiber dialysis using an Amicon DC2 unit and an H1P5-20 cartridge having a 5000 molecular weight cutoff instead of concentration by ammonium sulfate precipitation, (iv) application of the concentrated heated supernatant immediately on a column of Sephadex G-50-80 (11 × 100 cm equilibrated with 0.5% NH_4HCO_3, pH 7.8) instead of on a DEAE-cellulose column, and (v) use of the latter column equilibrated at pH 4.79 as the final step. Preparations of the purified protein had a specific activity of 77 ± 10 nmol/mg, migrated as a single component on polyacrylamide gels containing sodium dodecyl sulfate and on exclusion chromatographic columns, and had amino acid compositions appropriate to the purified protein (Holmgren & Reichard, 1967). No differences were detected in the properties of thioredoxin purified from *E. coli* B and from the strain that overproduces the protein. The yield of purified thioredoxin ranged from 35% to 40% of the enzyme in the initial extract, which represents a doubling of the yield obtained with the original purification procedure.

The chemicals Gdn-HCl, ethylene glycol, and the analogues of tyrosine and tryptophan used as fluorescence models were purchased from Heico, Fisher Scientific, and Sigma Chemical Co., respectively. Concentrations of stock solutions of Gdn-HCl were obtained from refractive index measurements while concentrations of stock solutions of the fluorescence models were obtained from absorbance measurements.

Equilibrium Measurements. Viscosity measurements were made by using a Cannon Ubbelohde viscometer having an outflow time for distilled water of 55.45 ± 0.12 s and protein samples having a concentration of 3.7 mg/mL.

Perturbation difference spectra were obtained with a Cary Model 17 recording spectrophotometer. Sample and reference solutions were placed in tandem cells whose cylindrical compartments each had an optical path of 10 mm. Protein and the perturbant ethylene glycol were placed in the same compartment in the sample cell but in different compartments in the reference cell. Perturbation spectra of the model chromophores were fit with the perturbation spectra of the protein by a linear search to obtain the smallest sum of the squared residuals between the two spectra.

Fluorescence spectra were obtained with an Hitachi Model MPF-2A recording spectrofluorometer. Samples were placed in square quartz cells having an optical path of 10 mm. The cells were placed in a hollow brass cell holder through which thermoregulated water was circulated; a Neslab Model RTE-9 refrigerated bath was used. Routine measurements were made by using an excitation wavelength of 295 nm, an excitation slit of 6, an emission slit of 8, and a sensitivity of 3. The analog signal was digitized and averaged with an IBM Instruments CS-9000 computer equipped with an A/D board.

Circular dichroic spectra were obtained with a Cary Model 60 CD spectropolarimeter, cylindrical cells having an optical path of 10 mm, a full scale of 0.1°, and a time constant of 0.3 s. The recorder trace from dichroic measurements at 219 nm was digitized and averaged with a Hewlett-Packard Model 7225B plotter interfaced to the IBM computer.

Kinetic Measurements. Stopped-flow fluorescence measurements were obtained with a Durrum Model D-110 spectrometer having an instrumental dead time of 6 ms. The mixing syringes and the optical cell block were bathed with circulating water maintained at 25 °C. The quartz observation cell has an excitation path length of 16 mm and an emission path length of 2 mm. An excitation wavelength of 295 nm and a slit of 4 mm were used, corresponding to a dispersion of 12 nm. The photometer was placed at a right angle to the excitation beam and the emitted light passed through a Corning 0-54 filter which transmits less than 10% of 305-nm light and more than 80% of 330-nm light. The output from the photometer was digitized with a Nicolet Model 3091 oscilloscope having 12-bit resolution and a storage capacity of 4000 points. The digitized data were delivered to a DEC Model 11/780 VAX computer and analyzed by a program developed by M. Dunn (University of California, Riverside) based on a series of FORTRAN subroutines for nonlinear least-squares curve fitting (Bevington, 1969). The program facilitates editing, averaging, plotting, and fitting of kinetic data. The kinetic data for thioredoxin were analyzed by using eq 1 for decreasing fluorescence intensity and eq 2 for increasing fluorescence intensity, where $y(t)$ is the fluorescence amplitude at time t, n is the number of kinetic phases, B_i is the change in fluorescence intensity associated with each kinetic phase, and τ_i is the relaxation time of each kinetic phase. The value of n giving the minimal χ^2 value and minimal sum of squared residuals between simulated and observed data was selected. The amplitude of each phase α_i was calculated by

$$y(t) = A + \sum_{i=1}^{n} B_i e^{-(t/\tau_i)} \quad (1)$$

$$y(t) = A + \sum_{i=1}^{n} B_i [1 - e^{-(t/\tau_i)}] \quad (2)$$

$$\alpha_i = B_i / \sum_{i=1}^{n} B_i \quad (3)$$

Kinetic measurements were also obtained by manual mixing as opposed to stopped-flow mixing. Protein samples were diluted in the optical cell and mixed by inversion to give a dead time of 30 s. Fluorescence measurements were made with the Hitachi spectrofluorometer, 295-nm excitation and 350-nm emission. The fluorescence signal was digitized by using a conversion rate of 3 s/point, and a total of 200 points was collected. The digitized data were analyzed as described above. Ellipticity measurements were obtained with the Cary spectropolarimeter at 219 nm.

Results

All measurements were performed with solvents containing 50 mM phosphate buffer adjusted to pH 7.0, thioredoxin having its single disulfide intact, and vessels thermostated to 25 °C unless noted otherwise. Stock solutions of denatured thioredoxin were equilibrated in concentrated Gdn-HCl prior to measurement.

Equilibrium Measurements. Native thioredoxin has a reduced viscosity of 3.6 mL/g, a value characteristic for small globular proteins. Addition of Gdn-HCl to 2 M does not increase the value of the reduced viscosity of the protein, but addition of 4 M denaturant increases the value to 13.0 mL/g. Reduction of the single disulfide with dithiothreitol in the presence of 4 M denaturant increases the reduced viscosity further to a value of 15.6 mL/g. We found that this latter value compares favorably with a reduced viscosity of 16.2

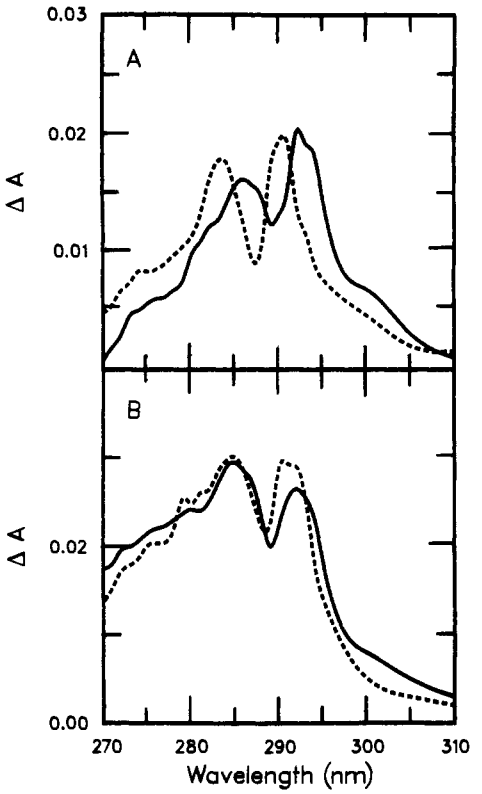

FIGURE 1: Solvent perturbation difference spectra. (A) Native oxidized thioredoxin. The solid line is the spectrum observed for a protein solution 84 μM in both tryptophan residues and tyrosine residues. The dashed line is the spectrum calculated for a solution containing 59 μM *N*-acetyltryptophan ethyl ester and 38 μM *N*-acetyltyrosine ethyl ester. (B) Denatured oxidized thioredoxin. The solid line is the spectrum observed for a protein solution in 4 M Gdn-HCl that is 84 μM in both tryptophan residues and tyrosine residues. The dashed line is the spectrum calculated for a solution containing 84 μM *N*-acetyltryptophan ethyl ester and 105 μM *N*-acetyltryrosine ethyl ester in 4 M Gdn-HCl. All protein and model chromophore solvents contained 50 mM phosphate buffer, pH 7.0. The solvent perturbant was 20% ethylene glycol.

mL/g expected for a randomly coiled polypeptide containing 108 residues using the equation of Tanford et al. (1967). The approximately 15% increase in reduced viscosity resulting from reduction of the single disulfide bond is similar to that observed for other proteins containing 1 disulfide per 100 residues (Tanford, 1968).

The near-ultraviolet solvent perturbation difference spectrum of native thioredoxin in 20% ethylene glycol is shown in Figure 1A. The profile of this spectrum fits well with that calculated for exposure of 1.4 model tryptophan residues and 0.9 model tyrosine residues. The 2-nm red shift of the perturbation spectrum of the model relative to the protein is commonly observed when examining native proteins. The presence of 4 M Gdn-HCl enhances the solvent perturbation difference spectrum as shown in Figure 1B. The profile of the denatured protein fits well with that expected for 2.0 model tryptophan and 2.5 model tyrosine residues as shown in Figure 1B. Thus, both tryptophan residues and both tyrosine residues in the protein appear to be exposed to the solvent in 4 M Gdn-HCl. It is likely that the contribution of other protein chromophores such as the phenylalanine residues and the disulfide accounts for the overprediction of tyrosine perturbation beyond the two residues present in the molecule.

Solutions of thioredoxin were subjected to 295-nm irradiation in an attempt to preferentially excite the two tryptophan residues in the protein as opposed to the two tyrosine residues. The emission spectrum of the native protein shown in Figure 2A has a single maximum at 342 nm, a value in the range anticipated for tryptophan residues. However, the area under the emission spectrum of the native protein is significantly smaller than that observed for an equimolar (in tryptophan residue) concentration of the model residue *N*-acetyltryptophan ethyl ester. Repetitive measurements indicate that the emission spectrum of the native protein is 31 ± 2% that of an equivalent concentration of the model. The presence of 6 M Gdn-HCl markedly increases the area of the protein emission spectrum and shifts its maximum to 350 nm as shown in Figure 2A. Repetitive measurements indicate that the area of the emission spectrum of the protein in 6 M Gdn-HCl is 87 ± 4% that of an equivalent concentration of the model in the same solvent. Since the intensity of the emission spectrum of both the protein and the model is proportional to its area, we observed the effect of changes in concentration of Gdn-HCl on the intensity of tryptophan fluorescence measured at 350 nm. As shown in Figure 2B, the emission intensity at 350 nm exhibits a sharp reversible transition centered at 2.5 M denaturant. This transition is steeper with a somewhat lower midpoint than reported previously (Holmgren, 1972), which we ascribe to correction by the model of the dependence of tryptophan emission intensity on Gdn-HCl concentration as seen in Figure 2A. Heating solutions of thioredoxin to 65 °C in the presence of excess concentrations of denaturant does not increase the tryptophan fluorescence of the protein relative to the model similarly treated. We conclude that the small quenching of thioredoxin tryptophan fluorescence in excess denaturant does not have a conformational origin but likely results from the proximity of the two tryptophan residues located at positions 28 and 31 to the disulfide bond linking cysteine residues 32 and 35.

The far-ultraviolet circular dichroic spectra of native and denatured thioredoxin shown in Figure 3A are similar to those previously observed by Reutimann et al. (1981). The profile of the dichroic spectrum of the native protein is characteristic for a protein with substantial α/β structure while the profile observed in 6 M Gdn-HCl is characteristic for structureless homopolymers in denaturing salts (Tiffany & Krimm, 1969). The dependence of the ellipticity observed at the minimum in the native dichroic spectrum at 219 nm on the concentration of Gdn-HCl describes a cooperative reversible transition centered at 2.5 M denaturant as shown in Figure 3B. The observed dependence of ellipticity measurements and that of tryptophan fluorescence measurements on Gdn-HCl concentration are compared in Figure 4. Both probes of structure appear to describe a common transition represented by the line drawn in the figure. Analysis of the common transition in terms of a two-state model without assumptions about binding of denaturant to the protein (Schellman, 1978) indicates that the native conformation has a free energy of stabilization in the absence of denaturant of 7.3 kcal/mol, a value typically observed for small globular proteins.

Unfolding Kinetic Measurements. As was the case for the equilibrium measurements, all solutions contained 50 mM phosphate, pH 7.0, as the buffer. Unfolding measurements of the oxidized protein were initiated by mixing thioredoxin equilibrated in 2 M Gdn-HCl with an equal volume of 6 M Gdn-HCl. This mixing procedure, termed 2-fold dilution, results in the observation of the unfolding of thioredoxin in 4 M Gdn-HCl. As shown in Figure 4, only completely denatured thioredoxin should be populated at equilibrium in this concentration of denaturant.

Stopped-flow measurements indicate that fluorescence intensity rapidly increases upon unfolding thioredoxin as shown

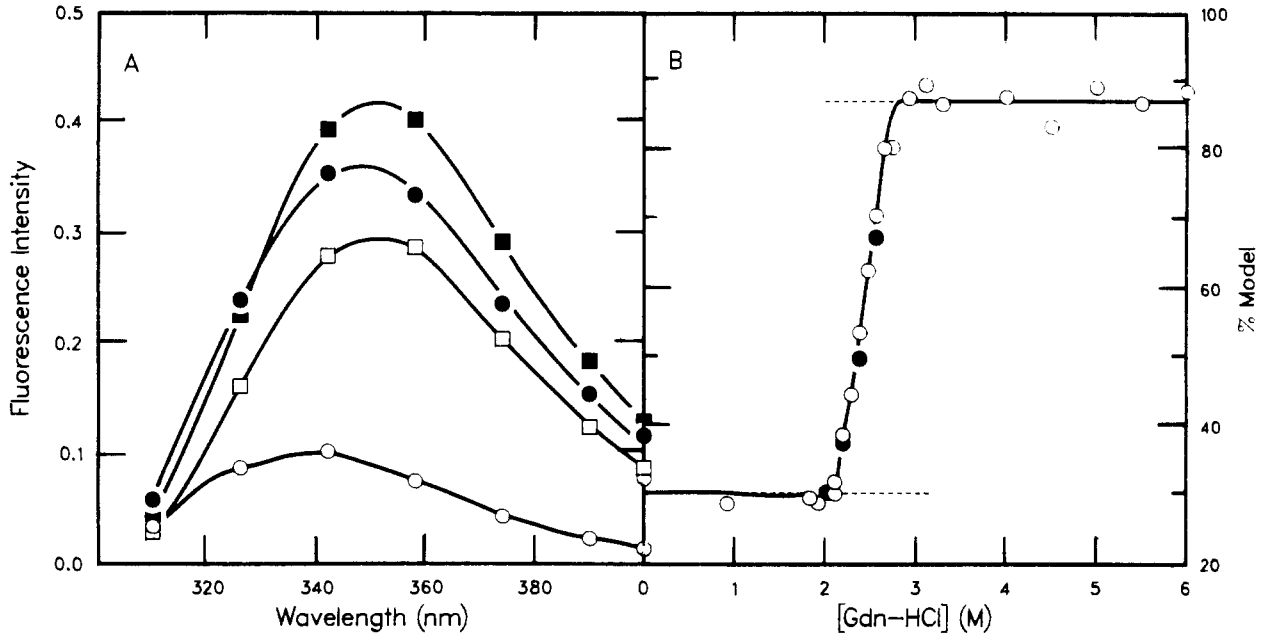

FIGURE 2: Fluorescence emission measurements. (A) Spectra. Solutions of oxidized thioredoxin (circles) and *N*-acetyltryptophan ethyl ester (squares) each 8 μM in tryptophan were subjected to 295-nm excitation. The open symbols were obtained with 50 mM phosphate, pH 7.0, as the solvent, and the filled symbols were obtained with the same solvent containing 4 M Gdn-HCl. (B) Dependence on denaturant concentration. A series of solutions of oxidized thioredoxin and of *N*-acetyltryptophan ethyl ester each 8 μM in tryptophan were equilibrated with variable concentrations of Gdn-HCl. The emission intensity of each sample at 350 nm was determined by using 295-nm excitation. The emission intensity of the protein is expressed as its percentage of the intensity of the model tryptophan chromophore measured in the same solvent. Each experimental value represents an average of triplicate samples. Values shown as open circles were obtained by dilution of a stock solution of native protein while values shown as filled circles were obtained by dilution of a stock solution of protein denatured in 6 M Gdn-HCl. All solutions were 50 mM in phosphate buffer, pH 7.0.

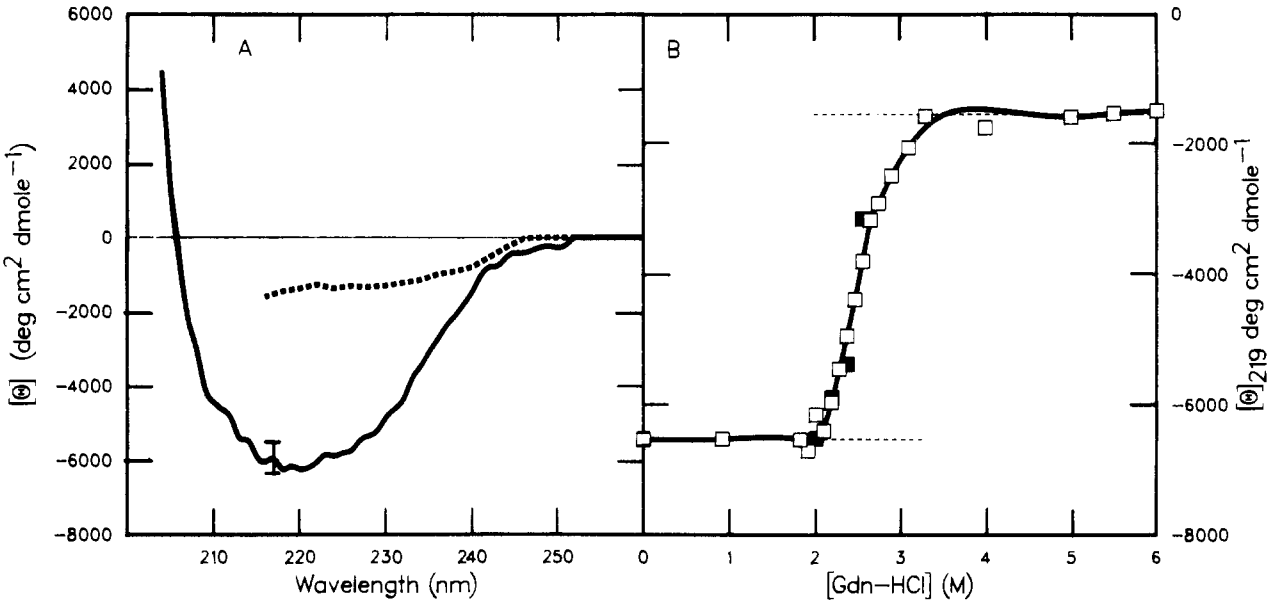

FIGURE 3: Circular dichroic measurements. (A) Spectra. The far-ultraviolet dichroic spectra of a 4 μM solution of oxidized thioredoxin observed in 50 mM phosphate buffer, pH 7.0, in the absence (solid line) and presence (dashed line) of 6 M Gdn-HCl are shown. (B) Dependence on denaturant concentration. A series of 4 μM solutions of oxidized thioredoxin in 50 mM phosphate buffer, pH 7.0, were equilibrated with variable concentrations of Gdn-HCl. The ellipticity values shown at 219 nm each represent an average of triplicate values. The open squares indicate values obtained by dilution of a stock solution of the native protein while the filled squares represent values obtained by dilution of a stock solution of protein denatured in 6 M Gdn-HCl.

in Figure 5A. Data collected in the first 10 s after mixing can be fit with high precision to a single exponential having the relaxation time shown for the fast unfolding phase in Table I. This phase must result from a unimolecular process since neither the relaxation time nor the amplitude is influenced by changes in protein concentration within the range 2–16 μM. Extrapolation of the intensity of the fast phase to zero unfolding time generates a value identical with that observed for the folded protein in 2 M Gdn-HCl. Thus it is unlikely that any significant amount of the increase in the fluorescence intensity accompanying the unfolding of thioredoxin occurs during the instrumental dead time. Extrapolation of the single kinetic phase to infinite time predicts a fluorescence amplitude identical with the equilibrium value. Accordingly, all of the change in fluorescence accompanying the unfolding thioredoxin appears to occur in a single kinetic event. Ellipticity measurements at 219 nm indicate that all of the dichroic change accompanying unfolding is completed within the manual

Table I: Kinetic Measurements

x-fold dilution	mixing procedure	probe	fractional amplitude			relaxation time (s)		
			fast	slow	slowest	fast	slow	slowest
unfolding								
2-fold	stopped-flow	fluorescence	1.0			7.1 ± 0.2		
refolding								
2-fold	stopped-flow	fluorescence	0.10 ± 0.02	0.10 ± 0.03	0.80 ± 0.09	0.56 ± 0.23	18 ± 5	450 ± 50
10-fold	stopped-flow	fluorescence	0.14 ± 0.04	0.12 ± 0.02	0.74 ± 0.08	0.52 ± 0.23	9.3 ± 4	300 ± 60
2-fold	manual	fluorescence			0.79 ± 0.06			560 ± 50
2-fold	manual	ellipticity			0.81 ± 0.04			610 ± 90
10-fold	manual	fluorescence			0.77 ± 0.04			590 ± 60

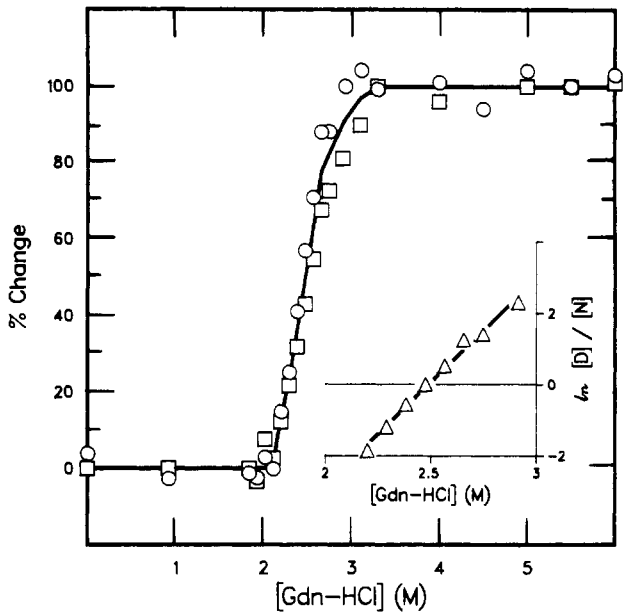

FIGURE 4: Comparison of fluorescence and ellipticity changes. The circles represent fluorescence emission values and the squares ellipticity values. The percentage change in each of these quantitites was calculated as $100(P_i - P_N)/(P_N - P_D)$, where P_i is the observed value at a given concentration of Gdn-HCl and P_N and P_D are the limiting values for the native and denatured forms shown by the lower and upper dashed lines, respectively, in Figures 2B and 3B. The inset to Figure 4 illustrates the least-squares fit of the mean values to a two-state model where [D] = $P_i - P_N$ and [N] = $P_D - P_i$.

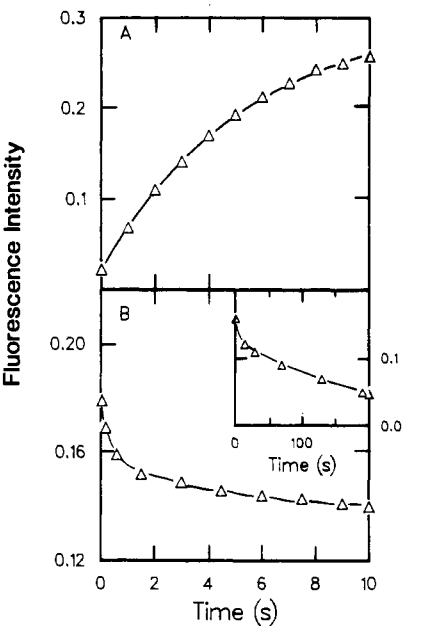

FIGURE 5: Stopped-flow measurements of fluorescence changes. The triangles represent experimental values, and the lines represent the relationship calculated by using one or more exponential terms in eq 1 and 2. Panel A illustrates the changes in fluorescence intensity accompanying unfolding of oxidized thioredoxin in 4 M Gdn-HCl. The line in the main body of the panel was calculated by using a single exponential. Panel B illustrates the decrease in fluorescence intensity accompanying refolding of denatured oxidized thioredoxin in 2 M Gdn-HCl with a 10-fold dilution. The lines in the main body of the panel and in the inset were calculated by using two exponentials. All measurements were obtained with 4 μM protein solutions in 50 mM phosphate buffer, pH 7.0. The instrumental settings for collection of the values in panels A and B were not identical.

mixing dead time of 30 s, suggesting that the single kinetic phase detected by stopped-flow fluorescence measurements represents complete unfolding of the molecule.

Refolding Kinetic Measurements. All solutions contained 50 mM phosphate buffer, pH 7.0. Refolding measurements were initiated by mixing solutions of thioredoxin equilibrated in 4 M Gdn-HCl either with an equal volume of buffer, a procedure denoted as 2-fold dilution, or with 9 volumes of 1.8 M Gdn-HCl, a procedure denoted as 10-fold dilution. In both procedures, the denatured protein is diluted to 2 M Gdn-HCl, a concentration in which the native protein should be the predominant form as shown in Figure 4.

Stopped-flow mixing measurements indicate that the decrease in fluorescence intensity accompanying refolding of thioredoxin in 2 M Gdn-HCl is multiphasic as shown in Figure 5B. A complete description of the kinetics of the total change in fluorescence intensity requires a minimum of three phases having the fractional amplitudes and relaxation times listed in Table I. Because of the large difference in the relaxation times of the fastest and slowest refolding phases, an accurate simultaneous fit of the observed data to three exponentials is not possible. The values for the two faster phases were obtained by fitting the data collected during the first 20 s after mixing with two exponentials. Extrapolation to zero mixing time predicts a value for the fluorescence intensity within experimental variation of the intensity of the denatured protein in 4 M Gdn-HCl, suggesting that a faster kinetic phase has not escaped detection. Values for the two slower kinetic phases were obtained by data collection for 400 s, deletion of the data collected in the first 4 s, and analysis of the remaining data using two exponentials. The values given for the common kinetic phase, the slow phase listed in Table I, include values obtained by using both phase pairings. The range of values observed for this phase is typical of that for any phase in either direction, suggesting that the procedure employed is appropriate to the data. The values shown for the unfolding phases in Table I are independent of protein concentration in the range 2–16 μM.

Spurious changes in absorbance have been observed in stopped-flow mixing measurements resulting from refractive index changes accompanying dilution of concentrated solutions of Gdn-HCl (Ikai et al., 1973). Such refractive index changes can be minimized by mixing a small volume of unfolded protein in concentrated denaturant with a much larger volume of dilute denaturant to generate the desired refolding conditions. As shown in Table I, the fractional amplitudes and

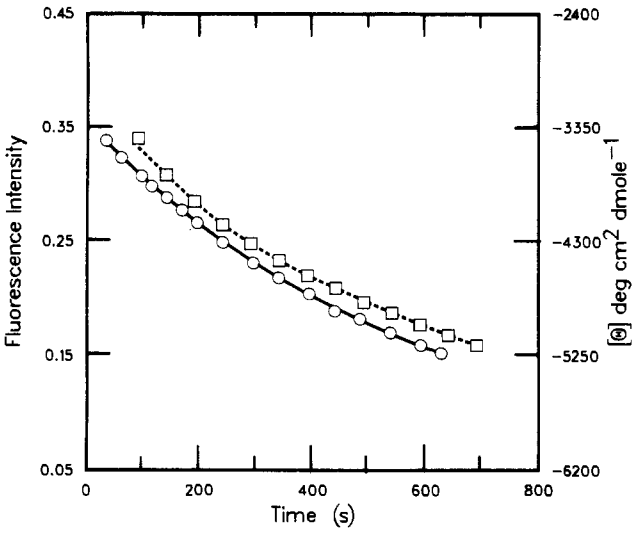

FIGURE 6: Refolding of oxidized thioredoxin observed by manual mixing measurements. The circles indicate observed fluorescence intensity values at 350 nm, and the solid line represents the relationship calculated by using a single exponential. The squares indicate observed ellipticity values at 219 nm, and the dashed line represents a relationship calculated by using a single exponential. The horizontal boundaries of the figure represent approximately the total change in signal expected for each observable during refolding.

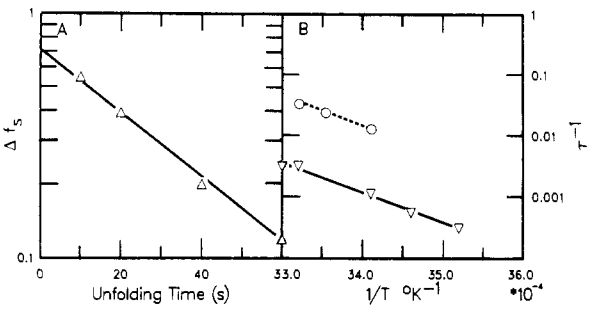

FIGURE 7: Aspects of the slowest phase in refolding. Panel A indicates the dependence of the amplitude of the slowest refolding phase on protein denaturation time. The experimental values are averages of three successive multimixing measurements. The term Δf_s is the difference in the amplitude of the slowest phase observed after incubation of the oxidized protein overnight in 4 M Gdn-HCl and the amplitude observed after incubation of the protein in 4 M Gdn-HCl for the indicated times prior to intiation of refolding. Panel B illustrates the dependence of the observed relaxation times on the temperature of the measurement. The circles represent the relaxation times for the generation of the protein exhibiting slowest phase refolding, and the inverted triangles represent the relaxation times for the slowest refolding phase itself.

relaxation times for each of the three kinetic phases observed during refolding of thioredoxin in 2 M Gdn-HCl using either 2-fold or 10-fold dilution are within experimental variation of identity. Accordingly, we suggest that the kinetic parameters shown in Table I are free of refractive index effects in either direction.

The large amplitude and long relaxation time for the slowest phase observed in refolding measurements by stopped-flow mixing should facilitate characterization of this phase by manual mixing procedures. A typical decrease in fluorescence intensity observed with a standard fluorometer following manual 2-fold dilution of denatured thioredoxin is shown in Figure 6. The decrease in fluorescence intensity fits very well with a single exponential having a relaxation time appropriate to that of the slowest phase observed by stopped-flow measurements, as shown in Table I. The good fit with a single exponential is not surprising since the two faster kinetic phases observed by stopped-flow mixing would be expected to have been essentially completed during the 30 s dead time for the manual mixing measurements. As shown in Table I, the fractional amplitudes observed for the slowest phase by stopped-flow fluorescence measurements and by manual mixing fluorescence measurements are the same within the experimental variability. Both the fractional amplitude and relaxation time of the slowest refolding phase observed in 2 M Gdn-HCl by manual mixing are independent of the concentration of Gdn-HCl in the denatured protein solution. Manual mixing measurements were also used to observe the increase in ellipticity of thioredoxin resulting from a 2-fold dilution of the protein denatured in 4 M Gdn-HCl. The increase in ellipticity observed after the 30 s mixing dead time fits well with a single exponential. As shown in Table I, the fractional amplitude and relaxation time of the single phase compare favorably with the values for the slowest phase observed by both stopped-flow and manual mixing fluorescence measurements. In contrast to the results described above obtained for the denatured oxidized thioredoxin, no change in either fluorescence intensity at 350 nm or ellipticity at 219 nm could be detected following 2-fold dilution by manual mixing of the denatured reduced and alkylated thioredoxin.

While it is virtually impossible to measure the temperature of the refolding solution in the fluorescence observation cell of the stopped-flow apparatus immediately after dilution of the denatured protein, it is easy to monitor temperature during and subsequent to manual mixing measurements. We find a maximal decrease of 0.5 °C in the temperature of the buffer solution located in the thermostated cell holder of the standard fluorometer upon addition of an equal volume of protein denatured in 4 M Gdn-HCl. The initial temperature, 25.0 °C, is recovered within 1 min after mixing. This initial decrease in temperature likely results from the cooling associated with dilution of concentrated solutions of Gdn-HCl. However, the relaxation time for the slowest phase observed in the refolding of oxidized thioredoxin, about 8 min, is long relative to the initial temperature fluctuation, which is over in 1 min and has a maximal deviation of no more than 0.5 °C. Further, a 10-fold dilution as opposed to a 2-fold dilution would be expected to produce a smaller thermal perturbation. As shown in Table I, identical kinetic constants are obtained from fluorescence measurements of the slowest refolding phase using either 2-fold or 10-fold manual dilution. Accordingly, we suggest that measurements of the slowest refolding phase obtained by using 2-fold manual dilution are free of temperature artifacts. As shown in Figure 7B, an Arrhenius plot of the temperature dependence of the reciprocal relaxation time of the slowest refolding phase is linear with an activation enthalpy of 22 kcal/mol. While the relaxation time of the slowest refolding phase is quite dependent on temperature, the fractional amplitude associated with this phase is independent of temperature.

The origin of protein exhibiting the slowest phase in refolding was examined by a manual multimixing protocol performed at 25 °C. Aliquots of oxidized thioredoxin were incubated in 4 M Gdn-HCl for variable time periods prior to 2-fold dilution with buffer and observation of the kinetics of the decrease in fluorescence intensity using a standard fluorometer. It was observed that the amplitude but not the relaxation time of the slowest refolding phase is dependent upon the incubation time in concentrated Gdn-HCl. This dependence generates a linear first-order plot, shown in Figure 7A, having a relaxation time of 42 s at 25 °C in 4 M Gdn-HCl. The relaxation time for the generation of the slowest refolding phase exhibits a small dependence on the concentration of

Gdn-HCl in the unfolding solution over the observable range from 4 to 6 M. This dependence predicts that the relaxation time for the generation of protein exhibiting the slowest phase in refolding would be 50 s in 2 M Gdn-HCl. The temperature dependence of the relaxation time in 4 M Gdn-HCl for the generation of the protein exhibiting the slowest phase in refolding yields a linear Arrhenius plot having an activation enthalpy of 23 kcal/mol as shown in Figure 7B.

Discussion

Solvent perturbation difference spectra indicate that about 70% of the indole chromophores of the two tryptophan residues are in contact with solvent in the native protein at neutral pH. Analysis of the surface of the crystallographic model of *E. coli* oxidized thioredoxin indicates that 42 Å^2 of the side chain of tryptophan residue 28 and 132 Å^2 of the side chain of tryptophan residue 31 are in contact with the solvent. These values correspond to 28% and 81% of the side chain area of a completely exposed tryptophan side chain as calculated by Lee & Richards (1971). Thus the average exposure of the two tryptophan side chains, 55%, corresponds fairly well with the average exposure measured by solvent perturbation given the limitations of each determination. The differential exposure of the two tryptophans in the crystallographic model correlates with proton NMR measurements (Holmgren & Roberts, 1976), which indicate that the two tryptophan residues are in different magnetic environments, and with chemical modification results (Holmgren, 1981), which demonstrate that tryptophan-31 is more reactive. The complete exposure of the two tryptophan chromophores in the presence of 4 M Gdn-HCl is in keeping with the remaining equilibrium measurements, which indicate that the protein is denatured in this solvent.

The fractional quenching of the fluorescence emission of the two tryptophan residues both in the native and in the denatured oxidized protein does not necessarily relate to the exposure of their indole chromophores but to their proximity and orientation to groups that can quench fluorescence. Prominent among such groups in oxidized thioredoxin is the disulfide bond linking cysteine residues 32 and 35 whose center is about 7 Å from the center of the indole chromophores of both tryptophan-28 and tryptophan-31 in the crystallographic model. Consistent with this view is the observation (Holmgren, 1972) that the tryptophan fluorescence intensity of thioredoxin increases 3-fold upon reduction of the disulfide, an observation confirmed by ourselves. In the denatured protein, it is reasonable to assume that the indole chromophore of tryptophan-31 would be closer on average to the disulfide linking positions 32 and 35 than would the indole of tryptophan-28. Accordingly, it may be surmised that the fractional quenching of tryptophan fluorescence observed for the denatured protein preferentially involves tryptophan-31. This being the case, the increase in tryptophan fluorescence emission accompanying denaturation would suggest a larger fractional contribution from tryptophan-28.

The correlation of changes in tryptophan fluorescence emission with changes in far-ultraviolet ellipticity at equilibrium suggests that changes in tryptophan fluorescence observed by stopped-flow measurements can be used to monitor the kinetics of the folding and unfolding of the polypeptide chain of oxidized thioredoxin. This assumption can be tested for the major kinetic phase in refolding owing to its very large relaxation time. As shown in Table I, both the fractional amplitude and relaxation time observed for the slow phase regain of secondary structure and for the regain of tertiary structure, as detected by far-ultraviolet ellipticity and by tryptophan fluorescence measurements, respectively, are identical within experimental variation. We will assume that this correspondence also applies to the faster kinetic phases detected by fluorescence measurements whose correlation with far-ultraviolet circular dichroic measurements cannot be established with available instrumentation.

While equilibrium measurements suggest that the major conformational transition of oxidized thioredoxin involves only two states, kinetic measurements demonstrate the occurrence of at least three phases in the refolding direction. This dilemma is commonly observed with a variety of proteins. One solution to the dilemma considers the denatured state to be populated by two or more configurational isomers, as opposed to conformational isomers, in slow exchange relative to the rate of protein folding. Brandts et al. (1975) have proposed that the configurational equilibrium involves the cis and trans isomers of peptide bonds. Rapid folding is proposed to originate from the fractional population of denaturated protein molecules that has all native-like isomers while slow folding is proposed to originate from an obligatory isomerization of one or more of the nonnative-like isomers prior to folding. At least two tests of this proposal are available. Since peptide isomerization is slow relative to protein folding and unfolding, it should be possible to demonstrate as one test that the slow phase in folding is generated in the denatured state by systematic variation of the interval between the initiation of protein unfolding and the initiation of protein folding. The multimixing measurements described here demonstrate that the population of thioredoxin molecules exhibiting slowest phase folding is generated in the denatured state with a relaxation time of 42 s at 25 °C in 4 M Gdn-HCl. A second test predicts that the activation energy of the slowest refolding phase as well as its generation should have a value characteristic for peptide isomerization, about 20 kcal/mol. The activation energy for the generation of thioredoxin molecules exhibiting slowest phase refolding has a value of 23 kcal/mol while the activation energy for the slowest folding phase itself is 22 kcal/mol.

Brandts et al. (1975) further propose that the peptide bonds most likely to accumulate significant populations of nonnative-like isomers in the denatured state involve peptide bonds in which the proline residues contribute the amide nitrogen. The relaxation time for the generation of the protein exhibiting slowest phase refolding, 42 s in 4 M Gdn-HCl at 25 °C, is in the range of values observed (Grathwohl & Wüthrich, 1976; Lin & Brandts, 1983) for isomerization of such proline peptide bonds. Recent refinement of the crystallographic model of oxidized *E. coli* thioredoxin indicates that the peptide bonds involving the amide nitrogen of proline residues 34, 40, 64, and 68 are trans while the peptide bond involving the amide nitrogen of proline-76 is cis (Brändén et al., 1983). Assuming that all proline peptide bonds are predominately trans in the denatured state, the presence of a cis proline peptide in a native conformation predicts that a slow phase should dominate the folding kinetics and that the relaxation time for the slow folding phase should be large. Both of these predictions are observed in the folding of thioredoxin. A mean value of 78% of the total folding amplitude occurs in the slowest phase, in keeping with a typical value of 75% trans isomer in the denatured state. Secondly, the relaxation time of the slowest phase has a mean value of 500 s, a value significantly larger than the range of 3–67 s observed for the slow phase refolding of a variety of small proteins containing between 1 and 9 proline residues (Stellwagen, 1979). In addition, the relaxation time for the cis to trans isomerization predicted from the multimixing measurements of thioredoxin, 227 s, is within a

factor of 2 of the mean relaxation time for the slowest folding phase. These comparisons indicate that the configurational isomerization of proline peptide 76 could account for the features observed for the slowest phase refolding of oxidized thioredoxin.

Several features of the crystallographic model of oxidized thioredoxin support this assignment. Proline-76 is located at the interface between the two domains of thioredoxin that constitute residues 1–72 and residues 73–108. It is likely that these domains have little individual stability in 2 M Gdn-HCl in the absence of the other domain since peptide fragments 1–73 and 74–108 have no detectable structural features in the absence of denaturant at neutral pH and room temperature (Slabý & Holmgren, 1979; Reutimann et al., 1981). If the peptide bond of proline-76 were trans rather than cis, it would be anticipated to perturb the surface of the C-terminal domain and to significantly weaken its complexation with the N-terminal domain. Since several of the atoms of the cis form of proline-76 are in van der Waals contact with the disulfide bond in the crystallographic model, it could also be anticipated that the conformational flexibility in the N-terminal domain accompanying reduction of the disulfide bond could provide for complexation of a C-terminal domain having a trans proline peptide bond at position 76. The observed total absence of the slowest kinetic phase in the refolding of the reduced protein is in keeping with such an expectation.

In spite of the attractiveness of assignment of the origin of the dominant slowest kinetic phase observed in the refolding of oxidized thioredoxin to proline-76, it must be recognized that the limited available data can be made compatible with a large number of scenarios involving not only other proline peptide bonds (Creighton, 1978) but also other conformational states. In an effort to select among these possibilities, we are currently developing the peptide cleavage and resolution procedures required for proteolytic determination (Lin & Brandts, 1983) of both the cis/trans ratio of individual proline peptide bonds in denatured oxidized thioredoxin and their isomerization rates.

Registry No. Gdn-HCl, 50-01-1; *N*-acetyltryptophan ethyl ester, 2382-80-1; *N*-acetyltyrosine ethyl ester, 840-97-1.

References

Bevington, P. R. (1969) *Data Reduction and Error Analysis for the Physical Sciences*, McGraw-Hill, New York.

Brändén, C.-I., Eklund, H., & Söderberg, B.-O. (1983) in *Functions of Glutathione: Biochemical, Physiological, Toxicological, and Clinical Aspects* (Larsson, A., Ed.) pp 223–230, Raven Press, New York.

Brandts, J. F., Halvorson, H. R., & Brennan, M. (1975) *Biochemistry 14*, 4953–4963.

Creighton, T. E. (1978) *J. Mol. Biol. 125*, 401–406.

Grathwohl, C., & Wüthrich, K. (1976) *Biopolymers 15*, 1462–1473.

Holmgren, A. (1968) *Eur. J. Biochem. 6*, 475–484.

Holmgren, A. (1972) *J. Biol. Chem. 247*, 1992–1998.

Holmgren, A. (1981) *Biochemistry 20*, 3204–3207.

Holmgren, A., & Reichard, P. (1967) *Eur. J. Biochem. 2*, 187–196.

Holmgren, A., & Roberts, G. (1976) *FEBS Lett. 71*, 261–265.

Holmgren, A., Söderberg, B.-O., Eklund, H., & Brändén, C.-I. (1975) *Proc. Natl. Acad. Sci. U.S.A. 72*, 2305–2309.

Ikai, A., Fish, W. W., & Tanford, C. (1973) *J. Mol. Biol. 73*, 165–184.

Laurent, T. C., Moore, E. C., & Reichard, P. (1964) *J. Biol. Chem. 239*, 3436–3443.

Lee, B., & Richards, F. M. (1971) *J. Mol. Biol. 55*, 379–400.

Lin, L.-N., & Brandts, J. F. (1983) *Biochemistry 22*, 553–559.

Lunn, C. A., Kathju, S., Wallace, B. J., Kushner, S. R., & Pigiet, V. (1984) *J. Biol. Chem. 259*, 10469–10474.

Pigiet, V. P., & Conley, R. R. (1977) *J. Biol. Chem. 252*, 6367–6372.

Reutimann, H., Straub, B., Luisi, P. L., & Holmgren, A. (1981) *J. Biol. Chem. 256*, 6796–6803.

Schellman, J. A. (1978) *Biopolymers 17*, 1305–1322.

Slabý, I., & Holmgren, A. (1979) *Biochemistry 18*, 5584–5591.

Stellwagen, E. (1979) *J. Mol. Biol. 135*, 217–229.

Tanford, C. (1968) *Adv. Protein Chem. 23*, 121–282.

Tanford, C., Kawahara, K., & Lapanje, S. (1967) *J. Am. Chem. Soc. 89*, 729–737.

Tiffany, J. L., & Krimm, S. (1969) *Biopolymers 8*, 347–359.